Numerical Study of Counter-rotating Waves in Hollow Rotating Detonation Chamber

Xiang-Yang Liu, Yan-Liang Chen, Zhi-Jie Xia, Jian-Ping Wang*
Center for Combustion and Propulsion, CAPT and SKLTCS, Dept. Mechanics and Engineering Science, College of Engineering, Peking University.
Beijing 100871, China

1 Extended Abstracts

The continuous detonation chamber (CDC) is a concept engine chamber using detonation as power source. Experimental researches have been done widely around the world by Wolański et al. [1], Rankin et al. [2] and Bykovskii et al. [3]. Numerical simulations of CDC with annular chamber were performed by Shao et al. [4], Schwer et al. [5] and Frolov et al. [6]. To resolve the problem of overheating of the inner cylinder in co-axial annular combustor model, a new model with hollow combustor was proposed by Tang et al. [7]. Various number of detonation fronts was observed under different fuel injection area ratios. To get closer to experimental conditions, Yao's simulation [8] used array-hole injection model which was close to actual injection structure. Multiple detonation fronts were observed in his simulation which was consistent with the multi-head experimental results.

This paper adopts the model of injection via array-hole in 3D numerical simulations of CDC with hollow combustor using the premixed stoichiometric hydrogen-air mixture. The calculation is based on the Euler equations coupled with a one-step Arrhenius chemistry model. The array-hole injection method is more practical than previous conventional simulations where ideal full-area injection model is used. Counter-rotating waves exist in flow field which are composed of obverse-rotating wave (ORW) propagating clockwise and reverse-rotating wave (RRW) propagating anticlockwise. Wave collision mode of these counter-rotating waves are investigated in this paper.

2 Physical and Numerical Models

The 3D Euler equations with source term are used as governing equations. Fifth-order weighted essentially non-oscillatory (WENO) scheme is used to split the flux vectors. The time integration is performed by the third-order total-variation-diminishing (TVD) Runge–Kutta method. One-step chemistry model parameters are the same as those Ma et al.[9] used. Outer wall radius of hollow chamber is R_{outer} = 6.0 cm and inner wall radius is R_{inner} = 3.0 cm (R_{inner} is just a dummy argument because there is no core cylinder in the hollow

Correspondence to: wangjp@pku.edu.cn

chamber). Outer region (R_{inner}<R<R_{outer}) on headwall is fresh gas intake area where the fresh premixed gas fed into the chamber by array of injectors. The inner region (R< R_{inner}) on headwall is solid wall. The structure of hollow combustor is illustrated in Figure 1a. The schematic of array-hole injection model is shown in Figure 1b. Premixed stoichiometric hydrogen-air mixture enters to the chamber through array-hole on headwall. Radius of holes is 2.5 mm and combustor length is 8.0 cm.

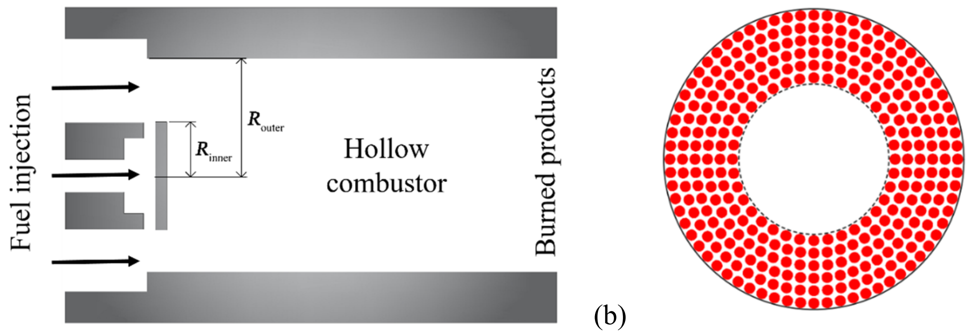

Figure 1. (a) Schematic of CDC with hollow combustor (b) Schematic of injection surface

3 The Counter-rotating Waves in Flow Field

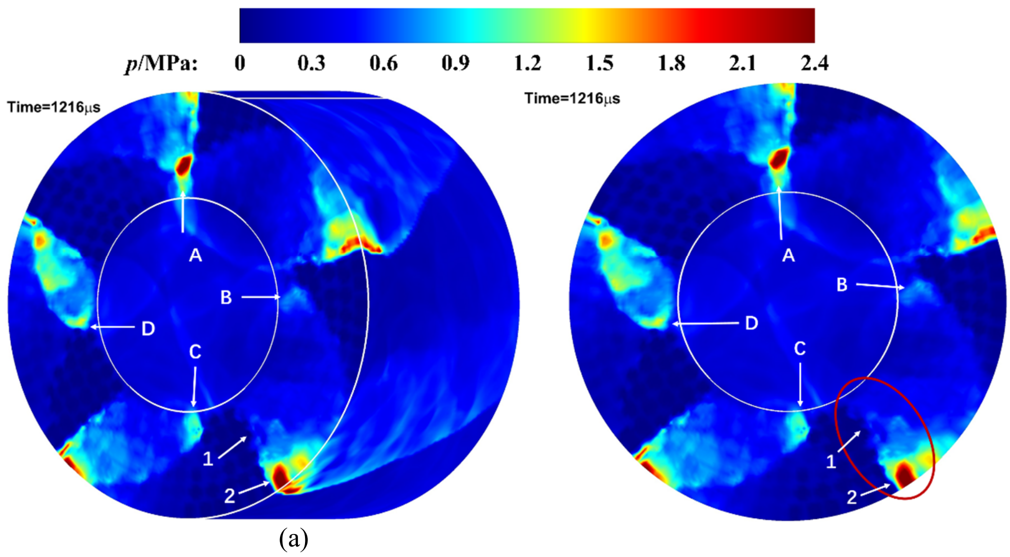

Figure 2. A/B/C/D represent the four reverse-rotating waves in the field. White circles represent for inner radius of combustor (R_{inner} = 3.0 cm). Gas intake area is R_{inner} < R < R_{outer}. (a) Pressure contours of the whole flow field (b) Pressure contours on headwall (X-Y plane, Z = 0 cm).

Figure 2. shows the pressure contours of flow field. These figures illustrate that there are five detonation waves propagate clockwise along outer wall of combustor. Four wave fronts propagate along the nominally inner wall in anticlockwise direction (Label A-D). They propagate in the opposite direction of outer detonation. We call these waves as reverse-rotating wave (RRW). Through careful observation of Figure 2, it can be found that the detonations along outer wall cannot penetrate the gas intake area. A clockwise

detonation in red ellipse (No. 2 in Figure 2b) decouples to shock wave (No. 1) at certain radial position. Therefore, the wave fronts propagating clockwise are detonations near outer radius but are shock waves near inner radius. This kind of wave fronts composed by detonation and shock is perpendicular to outer wall forming a planar clockwise wave front. We call them as obverse-rotating wave (ORW) corresponding to RRW. The ORWs and RRWs counter rotates in opposite direction and periodically collides with each other. Collision between counter-rotating waves is stable and reaches dynamic equilibrium status. For example, RRW-A collides with a ORW at the time shown in Figure 3 caused a high pressure and temperature area. After collision, new ORW and RRW will form and propagate continuously.

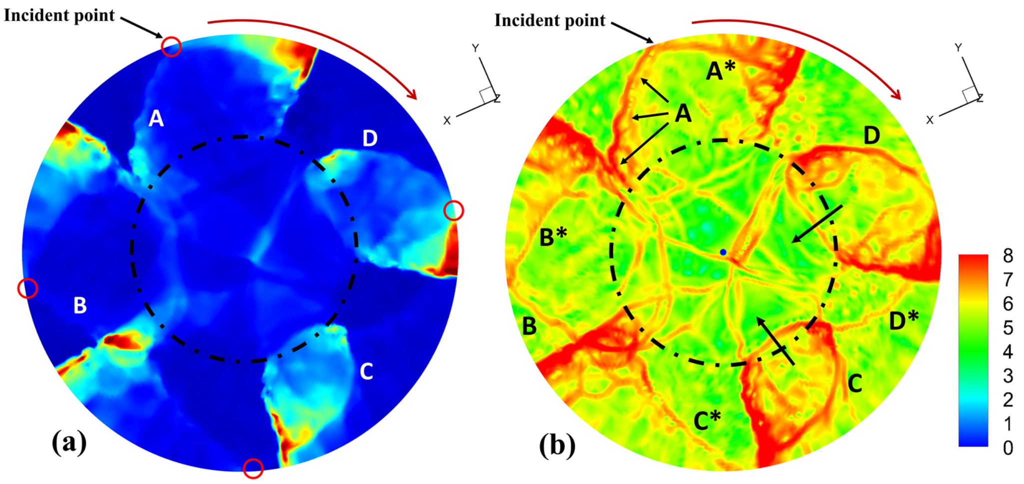

Figure 3. Complex wave structure on X-Y plane, z = 0.3 cm from bottom view (headwall is z = 0 cm) at 1258μs. Dash-dot circle represents for inner radius of chamber. Red arrows represent the propagation direction of detonations. (a) Pressure contour. (b) Logarithmic pressure gradient contour. Red area with high value of gradient represents for wave fronts. α represents for RRW front and α^* represents for reflect shock of RRW.

Logarithmic pressure gradient is calculated to distinguish complex reverse-rotating wave fronts in flow field. It can be found that the RRWs are curved in radial direction just like Wave-A in Figure 3a. The intensity of RRW around inner radius is highest and gradually weakens with increasing radius. RRWs can reflect on outer wall of combustor. From Figure 3b, it can be found that RRW-A reflects at incident point and forms a reflection shock wave A*. Moreover, the reflection shock of RRW does not disturb much by the ORWs. The reflect bow shock of RRW-C and D still exists even they go past the ORW structures. Incident points of these RRWs in Figure 3a are about asymmetric. Thus the complex reverse-rotating wave structures in flow field have good symmetry to axis of chamber. When collision happens, in addition to the formation of new RRWs and ORWs, a weak compression wave is generated and propagates into the inner region of combustor as shown by black arrows in Figure 3b. It is worth noting that fresh gas is injected into the combustor on outer region. Only combustion products exist at inner region. The energy that sustains the wave system is derived from fresh gas. Thus wave system mainly propagates at outer region ($R_{inner} < R < R_{outer}$). Compression waves at inner region have little effect to the evolution of flow field.

4 Wave Collision Mode on Different Slices

Contours are stretched in 2D along azimuthal direction as shown in Figure 4. Obverse-rotating wave (ORW) is traveling from left to right. Fresh gas is injected from the bottom.

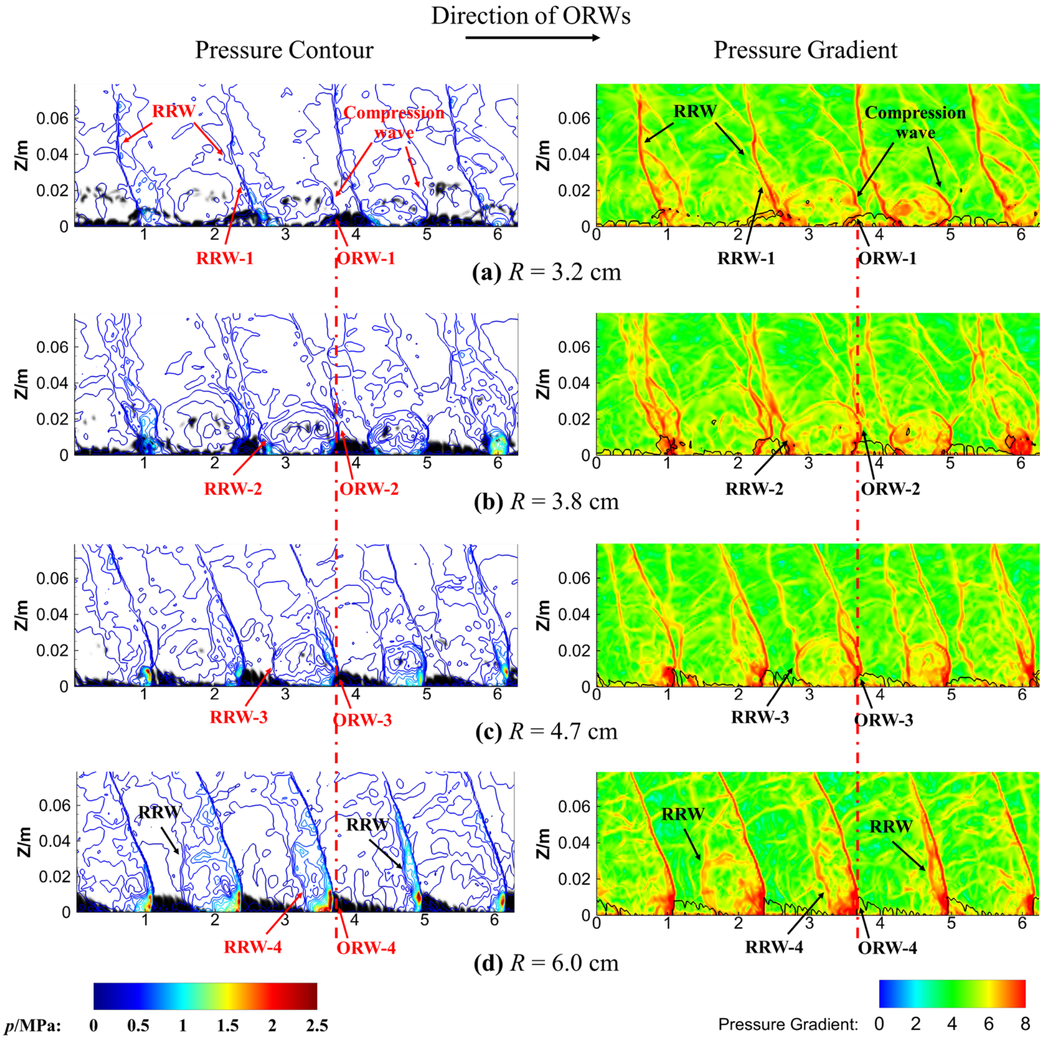

Figure 4. Left: Superposed maps of pressure contour and fresh gas distribution. Black area corresponds to fresh gas. Right: Pressure gradient. The line represents for outline of fresh gas.

Comparing the pressure contours at different radial position, it can be found that the strongest part of ORW is on the outer wall of combustor which is strengthened by the curvature of concave outer wall (Figure 4d). Five detonation waves with clearly distinguishable oblique shock wave propagate clockwise. Detonation front is sharp, straight and perpendicular to the headwall. The RRWs at this position is weak and have little effect to the propagation of detonations. Their structure can be investigated in pressure gradient contour. Wave intensity of ORWs decreases as radius goes down. The disturbance effect of RRWs on clockwise detonations begins to show up at around R = 4.7 cm. Detonation wave fronts are distorted under the collision of RRWs (Figure 4c). The oblique shock wave connected to detonations are weaker compared with R = 6.0 cm. At certain radial position around R = 3.8 cm, the detonation part of ORW decouples to ordinary shock wave. The strength of ORW and RRW are comparable to each other. Near the nominally inner radius, RRWs become dominant and have the delicate symmetry along the axis of combustor as shown in Figure 4a. ORWs degenerate to weak compression waves which is weaker than RRWs. Red dash-dot line in Figure 4 represents for a ORW. The positions of the ORW front on different radii are almost the same, 3.6 rad at

R=3.2 cm and 3.7 rad at R=6.0 cm. The ORWs are perpendicular to outer wall. The weakening of ORW from outer to inner wall is corresponding to the enhancement of RRW. The enhanced trend of RRWs can be observed from wave front RRW-4~1.

Figure 4 shows that the wave collision mode is different at various radial positions. Near the outer wall of combustor, strong detonations collide periodically with weak reverse shock waves as shown in Figure 4c and 4d causing detonation-to-shock collision process. Around slice R = 3.8 cm (Figure 4b), the counter-rotating shock waves with equal strength propagate in opposite direction causing shock-to-shock collision process. On slice R = 3.2 cm, it's also shock-to-shock collision process but the ORWs are pretty weak compared to RRWs. The opposite variation trend of RRW and ORW from inner to outer wall illustrates that they are interdependent with each other. A delicate equilibrium is built between them.

5 Conclusions

Array-hole injection model is used in 3D numerical simulations. The conclusions are as fallows:

1. For the wave structures propagating clockwise (ORW), they're detonations in periphery of the combustor but degenerate to shock waves in inner radius which are perpendicular to outer wall of combustor.
2. Besides the detonation waves, four reverse-rotating waves propagate along inner wall and are curved in the radial direction. The strength of RRWs gradually increase as the radius goes down and reaching peak values around the inner wall.
3. Periodic collisions happen between ORWs and RRWs at the outer region. Wave collision mode are different at different radial slices. Collision between counter-rotating waves is in a state of dynamic equilibrium.

Acknowledgments

The present study is sponsored by the National Natural Science Foundation of China (Grant No. 91741202).

References

[1] Kindracki J, Wolański P, Gut Z. (2011). Experimental research on the rotating detonation in gaseous fuels–oxygen mixtures. Shock Waves. 21(2):75-84.

[2] Rankin BA, Richardson DR, Caswell AW, Naples A, Hoke J, Schauer F. (2015). Imaging of OH* chemiluminescence in an optically accessible nonpremixed rotating detonation engine. 53rd AIAA Aerospace Sciences Meeting.

[3] Bykovskii FA, Zhdan SA, Vedernikov EF. (2006). Continuous spin detonations. Journal of Propulsion and Power. 22(6):1204-16.

[4] Shao Y-T, Liu M, Wang J-P. (2010). Numerical Investigation of Rotating Detonation Engine Propulsive Performance. Combustion Science and Technology. 182(11-12):1586-97.

[5] Schwer DA, Corrigan AT, Kailasanath K. (2014). Towards Efficient, Unsteady, Three-Dimensional Rotating Detonation Engine Simulations. 52nd AIAA Aerospace Sciences Meeting.

[6] Frolov SM, Dubrovskii AV, Ivanov VS. (2012). Three-dimensional numerical simulation of the operation of the rotating-detonation chamber. Russian Journal of Physical Chemistry B. 6(2):276-88.

[7] Tang X-M, Wang J-P, Shao Y-T. (2015). Three-dimensional numerical investigations of the rotating detonation engine with a hollow combustor. Combustion and Flame. 162(4):997-1008.

[8] Yao S, Han X, Liu Y, Wang J. (2016). Numerical study of rotating detonation engine with an array of injection holes. Shock Waves. 27(3):467-76.

[9] Ma F, Choi J-Y, Yang V. (2006). Propulsive Performance of Airbreathing Pulse Detonation Engines. Journal of Propulsion and Power. 22(6):1188-203.